Annals of Arid Zone 40(3): 233-250, 2001

Processes of Soil Erosion by Wind

L.J. Hagen

Wind Erosion Research Unit, USDA, ARS,
GMPRC, Wind Erosion Research 1515 College Ave, Manhattan, KS 66502, USA

Abstract: In the past, wind erosion has often been modeled as a series of lumped factors, with each factor embodying a number of individual erosion processes. During the last decade considerable progress has been made in formulating process equations that represent the individual sources and sinks for eroding soil. The objective of this report is to provide an overview of some of the wind erosion processes on agricultural lands. By considering two soil states (crusted and aggregated) along with the erosion processes, one can define the temporal soil properties of dry soils that control soil erodibility. These temporal properties include the dry stabilities, mass fractions and size distributions of mobile and immobile soil components, as well as surface roughness. The threshold friction velocities of bare soils also depend upon surface roughness and cover of immobile clods and crusts. The transport capacity of the suspension-size soil is several times larger than the limited transport capacity for the saltation and creep-size component of horizontal soil discharge. Thus, on large fields suspension discharge often exceeds saltation/creep discharge. Sources of saltation/creep discharge include entrainment of loose aggregates and abrasion of immobile clods and crust. Sinks for saltation/creep discharge include trapping by surface roughness, interception by standing biomass and breakage to suspension-size. Similarly, sources for suspension discharge include entrainment of loose aggregates, abrasion of clods and crust, and breakage of saltation/creep aggregates. Sinks for suspension include interception by standing biomass and deposition on downwind immobile surfaces. Wind tunnels have been used to directly measure the parameters for the individual wind erosion processes. Moreover, the individual processes can be assembled into physically-based wind erosion models that are applicable to a wide range of surface conditions.

Key words: Wind erosion, erosion processes, particulate, dust, soil, PM_{10}, $PM_{2.5}$.

The early work of Bagnold (1941) provided a firm basis toward understanding the processes involved in wind transport of loose, dry sand. Among the processes studied were effects of wind and particle interactions on threshold velocities and horizontal mass transport rates. Subsequent research on erosion mechanics of loose particles has expanded upon Bagnold's initial work (Anderson *et al.*, 1991). However, complex wind patterns and surface wetness still make predicting the transport of sand on dunes and on beaches a challenging research area (Van Dijk *et al.*, 1999; White and Tsoar, 1998; Gares, 1988).

Animal and human effects on agricultural lands in semi-arid and arid regions have often accelerated natural wind erosion. As

Contribution from USDA, ARS in cooperation with Kansas Agricultural Experiment Station, Contribution No. 02-114-J

a result, there has been considerable research aimed at predicting and controlling wind erosion on these lands (Chepil and Woodruff, 1963; Leys, 1999). However, agricultural land surfaces are generally more complex than bare, dry, loose sands. For these complex agricultural surfaces, researchers identified the major factors that influenced wind erosion. But the need to convey erosion prediction and controls in simplified models, led researchers to further lump the factors. These lumped factors included effects of soil erodibility, climate, surface roughness, field scale, and vegetation (Woodruff and Siddoway, 1965; Fryrear *et al.*, 1998).

In general, the lumped factors incorporate a number of wind erosion processes. This tends to obscure interactions among the processes and often requires calibration to field measurements before application (Saxton *et al.*, 2000). The widespread availability of computers now makes it feasible to consider individual processes in wind erosion prediction and control systems. As a result, several recent models of wind erosion have been oriented toward simulating individual erosion processes in desert lands (Marticorena and Bergametti, 1995; Draxler *et al.*, 2001) and on agricultural lands (Shao *et al.*, 1996; Hagen, 1999). This approach has two attractive features. First, individual processes can be defined to facilitate experimental parameter development in wind tunnels without the requirement for field calibration (Hagen, 2001c; Mirzamostafa *et al.*, 1998), and second, the processes can readily be combined to build complex models applicable to a wide range of surface conditions (Hagen *et al.*, 1999). Of course, field validation of models is still a much-needed part of comprehensive wind erosion research programs.

The purpose of this report is to provide an overview of wind erosion processes on agricultural lands. In this endeavor, we shall provide only brief comments on well-known results and focus on some of the lesser-known, but nevertheless important, processes associated with wind erosion. Areas that need additional research also will be briefly discussed.

Soil Surface Conditions

To facilitate understanding of erosion processes, it is useful to consider two general states of the soil surface. The surface may be composed of loose aggregates as exemplified by a newly-tilled surface. But the most common surface condition consists of an upper layer with a water-consolidated zone that has a partial cover of loose, mobile aggregates. These loose aggregates are often sand grains or water stable aggregates that are a result of raindrop impacts (Chepil and Woodruff, 1963). However, the loose aggregates may be absent from a crust created by snowmelt on the same soil. For this discussion, we shall refer to the entire water-consolidated zone as crust, although crust usually is defined as only the high density, upper portion of the consolidated zone. Obviously, strip tillage or other processes may create surfaces where both states are present. Crusted surfaces without a source of mobile aggregates to serve as abraders are generally stable, except under extreme winds (Marticorena *et al.*, 1997). Similarly, surfaces composed of loose, immobile aggregates may be stable.

Although efforts have been made to classify wind erodibility of various soils

Table 1. Temporal soil parameters that control wind erodibility of dry, bare soil

Parameters	Soil State	
	Crusted with loose cover	Loose aggregates
Dry aggregate stability by layer		
Mobile	X	X
Immobile	X	X
Roughness		
Random	X	X
Oriented	X	X
Crusted		
Mobile loose mass on top	X	
Crust (consolidated zone) thickness	X	
Aggregate size distribution by layer		
All soil layers		X
Layers below crust	X	
Rock volume fraction (>2 mm) by layer	X	X

(Chepil and Woodruff, 1963), the precision of the classification has been hampered because, as yet, there is not an accepted standard measurement for it. Some of the difficulties in defining a standard measure results from the fact that for a defined wind storm, the upwind and downwind ends of a field generally are subjected to different amounts of abrasion by saltating aggregates. Thus, locations on the same field have differing soil losses. Moreover, the soil conditions that control erodibility are temporal and depend upon both soil management and weather. However, by considering the erosion processes and the soil state, one can define measurable, temporal, soil parameters that control soil wind erodibility (Table 1). Using validated erosion models to integrate the effects of the temporal soil parameters on soil loss over time may prove to be the most efficient method to classify wind erodibility of soils.

The dry stability of immobile crusts and clods can be measured by crushing energy-meters (Boyd *et al.*, 1983; Hagen *et al.*, 1995). The range of the temporal distribution of the crushing energy also has been related to soil clay content (Skidmore and Layton, 1992). Stability of mobile, saltation-size aggregates (0.10-0.84 mm in diameter) is approximately nine times that of the immobile clods of the same soil as measured by impact breakage tests on a small number of soils (Mirzamostafa *et al.*, 1998). In the past, repeated sieving has been used as an aggregate stability indicator (Chepil and Woodruff, 1963). However, in tests (unpublished) we found that repeated sieving generally destroyed weak aggregates with a crushing energy <0.5 J kg^{-1}, but was largely insensitive to the stability range of stronger aggregates.

Medium-textured, crusted soils generally have lower wind erodibilities than similar uncrusted soils, but the dry stability of the crust is usually equal or less than that of the underlying clods (Chepil and Woodruff, 1963; Zobeck and Popham, 1992). Thus, the reduction in erodibility of crusted soils is likely caused by lower amounts of available mobile soil on the crust than among loose, surface aggregates. Loose soil on crusts can be sampled using vacuum devices (Zobeck, 1989), wind tunnels, or even a soft brush and pan. Relationships to predict the loose materials on crusts have been developed for a few soils (Potter, 1990).

In contrast, the reduction in roughness caused by rainfall or irrigation on sandy soils (Zobeck and Onstad, 1987) often leaves them more erodible than in their aggregated, pre-rain condition. Hence, rolling tined cultivators ("sand fighters") are often used after rain on these soils to restore some of the random roughness and shelter the mobile aggregates from the wind.

While wind erosion is a surface phenomenon, measurement of parameters in several soil layers is suggested, so that one can estimate the effects of soil disturbance. For example, disturbance of a desert pavement typically creates a highly erodible surface. In contrast, emergency tillage of crop land is often used to roughen and bring clods to the surface to reduce soil erodibility.

When estimating average soil erosion, it is important to determine the distribution of the soil temporal conditions, because, in general, amount of soil erosion is non- linearly related to the surface soil conditions, as illustrated by the example in Fig. 1. Thus, if one uses the average surface condition, 0.5, to estimate average relative erosion, the result is Y3avg = 0.11. However, if

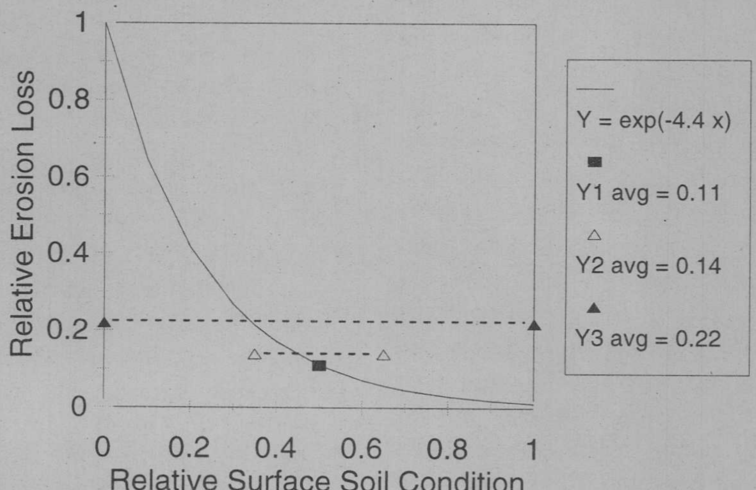

Fig. 1. Example illustrating effects of three distributions of relative soil surface condition on average erosion when the relationship between erosion loss and surface condition is non-lenear.

the surface conditions have a normal distribution (mean = 0.5, standard deviation = 0.15), then average erosion is Y2avg = 0.14. Finally, if surface conditions have a uniform distribution, the average relative erosion would be Y1avg = 0.22. When the wind speed distribution is also included in simulations, the non-linearity of erosion response to surface conditions increases further (Hagen, 1996). One may readily conclude from this example, that inputting only average soil conditions in erosion models may estimate erosion for the average soil condition, but may not estimate that which the model user may be seeking, namely, average erosion. Much additional research is needed to improve the understanding, distributions, and predictions of the soil temporal properties that control wind erosion.

Threshold friction velocities

The wind shearing stress or drag (τ) on the soil surface is related to the friction velocity (u_*) as

$$\tau = \rho (u_*)^2 \qquad ...1$$

where,

ρ is air density. Early experimental data demonstrated that the static threshold friction velocity (u_{*t}), where particle movement on a smooth bed of erodible particles began, depended on both particle diameter and density, as well as air density (Bagnold, 1941). Moreover, once erosion began on a surface with an unlimited source of particles, it would continue until the velocity was reduced below a dynamic threshold friction velocity, which was about 0.8 u_{*t}. Later measurements showed that interparticle cohesive force increased the u_{*t} of small particles and gravitational force increased u_{*t} of large particles above a minimum u_{*t}, which occurred for particle beds with diameters ranging from about 60 to 100 μm (Chepil, 1958; Iversen and White, 1982).

On erodible surfaces with a partial cover of uniformly distributed non-erodible elements, measurements show that drag on the surface is split between the protruding elements and the intervening erodible surface (Marshall, 1971; Lyles *et al.*, 1974). Frontal area of the protruding elements is the major variable controlling the drag partitioning. For this case, Raupach (1992) proposed an analytical formula that gave reasonable agreement with the measurements.

However, it is not feasible to determine frontal area on a bare soil surface with random distribution of both the non-erodible aggregates and surface heights. To overcome this difficulty, Marticorena and Bergametti (1995) proposed that

$$u_{*t}(D_p, Z_o, Z_{os}) = \frac{u_{*ts}(D_p)}{b(Z_o, Z_{os})} \qquad ...2$$

where,

D_p is the diameter of the erodible particles, and Z_o is the aerodynamic surface roughness.

The threshold friction velocity on a smooth bed (u_{*ts}), and its aerodynamic roughness (Z_{os}) are functions of D_p. The fractional values of the efficiency factor (b) were estimated using the empirical equation

$$b = 1 - \frac{\ln(Z/Z_{os})}{\ln[0.35(10/Z_{os})^{0.8}]} \qquad ...3$$

The values of b were highly correlated with the measured data of Marshall (1971) and Raupach (1992) on surfaces with a narrow

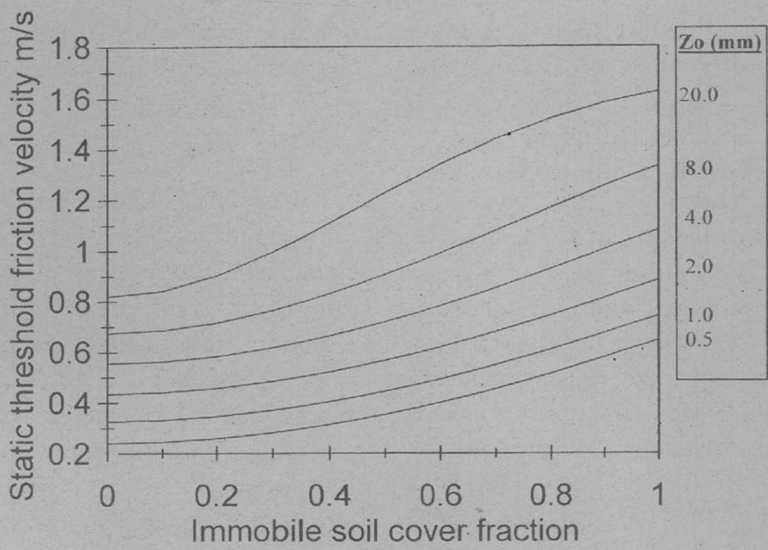

Fig. 2. Static threshold friction velocity as a function of immobile clod and crust cover on bare, dry soil for a range of aerodynamic

size range of erodible particles and uniform protruding non-erodible elements.

But there remain a number of difficulties in applying the preceding two equations to agricultural fields. The macro-roughness that determines Z_o is usually initiated by tillage and then modified by weathering forces (Zobeck and Onstad, 1987). Unfortunately, the macro-roughness is generally not well-correlated with the aggregate size distribution (Wagner and Hagen, 1992). Thus, the surface fraction covered by immobile soil aggregates or crust is not represented in the preceding equation. Obviously, there is a significant difference in threshold velocities between tillage ridges normal to the wind direction that are composed of mobile particles and the same ridge stabilized by a crust with a few mobile particles in the shelter between the ridges. The value to choose for D_p is also uncertain for soils with a distribution of erodible aggregate sizes. Draxler *et al*. (2001) slightly modified the equation to calculate b and further suggested that D_p should be assigned the mean soil aggregate diameter.

Currently, the WEPS erosion submodel (Hagen *et al*., 1999) uses an empirical family of curves to estimate u_{*t} on dry, bare, mineral soil of the form (Fig. 2),

$$u_{*t} = f(Z_o, F_c), \ F_c < 1.0 \qquad ...4$$

where,

F_c is fraction surface cover of immobile aggregates and crust >0.84 mm diameter. Minimum u_{*t} is set at 0.24 m s^{-1}.

Other factors also increase surface threshold velocities. Measurements show surface wetness (Saleh and Fryrear, 1995; McKenna-Neuman and Nickling, 1989) begins to increase threshold velocity at soil water contents well below plant wilting point.

Flat and standing biomass increase threshold velocities, as well as interact with the mobile soil aggregates (Hagen, 1996; Armbrust and Bilbro, 1997; Retta *et al.*, 1996).

Wind Erosion Transport Modes and Capacities

There are three modes of wind erosion transport. Creep-size aggregates (0.8-2.0 mm in diameter) roll along the surface in intermittent motion propelled by both wind gusts and saltation impacts. Saltation-size aggregates (0.1-0.8 mm in diameter) saltate (hop) along the surface, while suspension-size aggregates (< 0.1 mm in diameter) generally move above the surface with little surface contact. Obviously, the size limits in a given transport mode vary somewhat depending on wind speed and aggregate density.

It is useful to delineate between transport capacity for saltation/creep-size aggregates and suspension-size. To describe horizontal mass discharge data for saltation and creep transport capacity, a variety of equations have been derived (Greeley and Iversen, 1985). One of the most frequently used was developed by Lettau and Lettau (1978) and can be expressed as

$$q_{en} = C_s u_*^2 (u_* - u_{*t}) \quad ...5$$

where,

C_s is the saltation transport parameter (kg m^{-4} s^2), with a typical value of about 0.3 or more for surfaces armored with stones, u_* is friction velocity (m s^{-1}), and u_{*t} is dynamic threshold friction velocity (m s^{-1}). The saltation/creep discharge (q_{en}) from a smooth field (aerodynamic roughness 0.003 m) with friction velocity equal 0.74 m s^{-1} (wind speed equal 15 m s^{-1} at 10 m height) would be 0.08 kg m^{-1} s^{-1}. As surface roughness and shelter by immobile cover increases, u_{*t} also increases resulting in lower transport capacities for saltation and creep-size aggregates. When the immobile shelter is sufficient to prevent incoming saltation from impacting mobile aggregates, measurements show u_{*t} increases from the dynamic to static threshold (Hagen and Armbrust, 1992).

In contrast to the limited transport capacity for saltation/creep, the transport capacity for suspension is much larger and can be considered nearly unlimited on typical eroding fields. To illustrate, consider the following example based on concentration and visibility measurements in a series of dust storms (Chepil and Woodruff, 1957). The average concentration, C_o (mg m^{-3}) at 1.83 m height as a function of visibility, V (km) was measured as

$$C_o = \frac{56}{V^{1.25}} \quad ...6$$

The average vertical concentration profile, C(z) followed a power law, and can be represented as

$$C(z) = C_o \left(\frac{Z}{1.83}\right)^{0.28} \quad ...7$$

where,

z is height (m) above the surface.

The suspension discharge, qss (kg m^{-1} s^{-1}), for any visibility can then be estimated as

$$qss = \int_{z_o}^{z_1} C(0.1)u(z)dz + \int_{z_1}^{z_2} C(z)u(z)dz \quad ...8$$

For this example, the wind speed was 15 m s^{-1} at 10 m height, while u(z) represented the log-law vertical wind speed profile. The dust concentration was uniform in the active

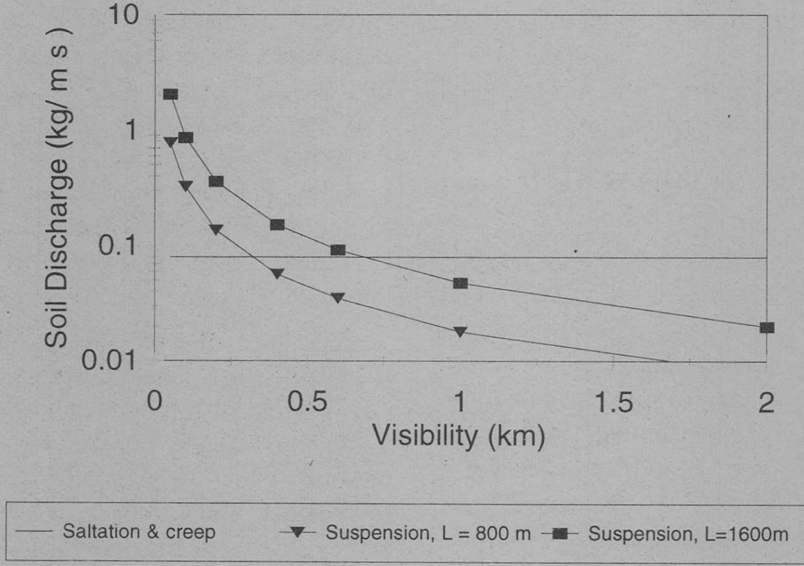

Fig. 3. Maximum soil discharge at wind speed of 15 m s^{-1} for saltation and creep compared to a range of suspension discharge rates corresponding to a range of visibilities at 1.83 m height.

saltation zone extending from z_o to 0.1 m, and the slope of the diffusion zone was estimated as 1:50 so that z_2 was 16 m and 32 m at 800 and 1600 m downwind, respectively. For example, results show that as visibility is reduced below about 0.5 km, one can expect the suspension transport to exceed the maximum saltation and creep transport (Fig. 3). Moreover, at low visibilities where vehicle traffic is impeded, suspension transport greatly exceeds the saltation and creep transport from a single field.

Saltation and Creep Discharge

In this section, we shall consider the individual processes that control the saltation/creep discharge. Based on conservation of mass in a control volume (Fig. 4), a one-dimensional, quasi-steady state equation for the physical processes involved in saltation/creep is:

$$\frac{dq}{dx} = Gen + Gan - Gss_{bk} - G_{tp} \qquad ...9$$

where,

q is horizontal saltation/creep discharge (kg m^{-1} s^{-1}), x is downwind distance from non-erodible boundary (m), and terms on the right hand side of Eq. 9 are all net vertical fluxes (kg m^{-2} s^{-1}). G_{en} is flux from emission of loose aggregates, G_{an} is flux from abrasion of surface clods and crust, Gss_{bk} flux of suspension aggregates from breakage of saltation/creep aggregates, and G_{tp} is flux from trapping of saltation/creep aggregates. Each of the vertical fluxes represents either source or sink terms in the control volume and can be estimated by the equations that follow. The net emission source term for loose aggregates is

$$G_{en} = (1 - SFss_{en})\ C_{en}\ (q_{en} - q) \qquad ...10$$

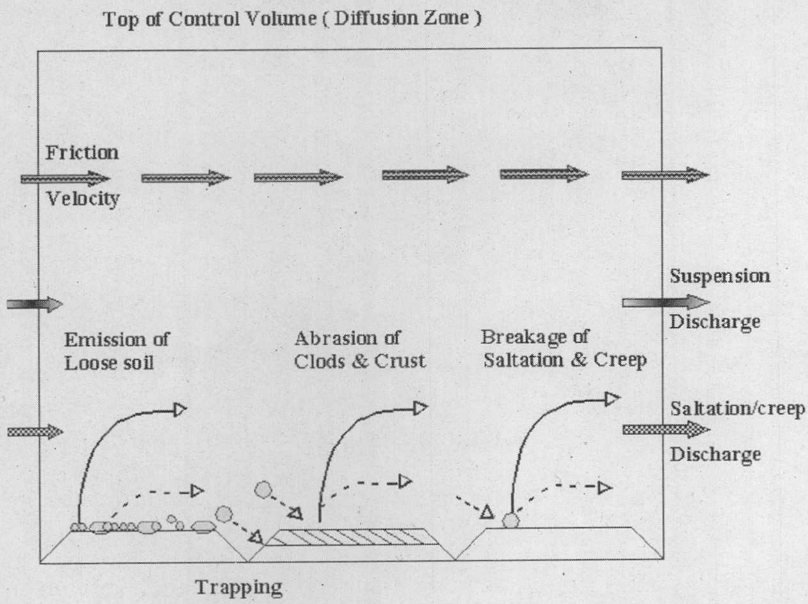

Fig. 4. Schematic of a control volume on a bare, rough, eroding surface illustraing friction velocity as the driving force and sources and sinks for saltation/creep (dashed lines) and suspension (solid lines) discharge.

where,
$SFss_{en}$ is mass fraction of suspension-size (<0.10 mm) among loose aggregates (<2.0 mm diameter), C_{en} is coefficient of emission (m^{-1}), and q_{en} is transport capacity (kg m^{-1} s^{-1}).

A typical value for C_{en} on a loose, bare field is about 0.06 m^{-1}, and values for other conditions have been reported (Hagen, 1995). At transport capacity, dq/dx equals zero. However, the emission and/or abrasion flux typically continue over the entire field to satisfy the discharge lost to breakage and/or trapping. In this case, the actual transport capacity must be some value of q that is less than q_{en}.

The suspension-size aggregates are assumed to be mixed intimately with the saltation/creep-size and emitted with them. Although the suspension-size aggregates absorb part of the aerodynamic and impact energy (represented by the emission coefficient) in order to rise from the surface, they do not contribute toward reaching the transport capacity of saltation/creep. Hence, they are subtracted from the total emission of loose aggregates in Eq. 10.

The net source term for entrainment of saltation/creep aggregates abraded from immobile clods and crust by impacting saltation/creep is

$$G_{an} = (1 - SFss_{an})\left[\sum_{1}^{2} (F_{ani}\, C_{ani})\, q\right]\left(\frac{q_{en} - q}{q_{en}}\right) \quad ...11$$

where,
$SFss_{an}$ is mass fraction of suspension-size

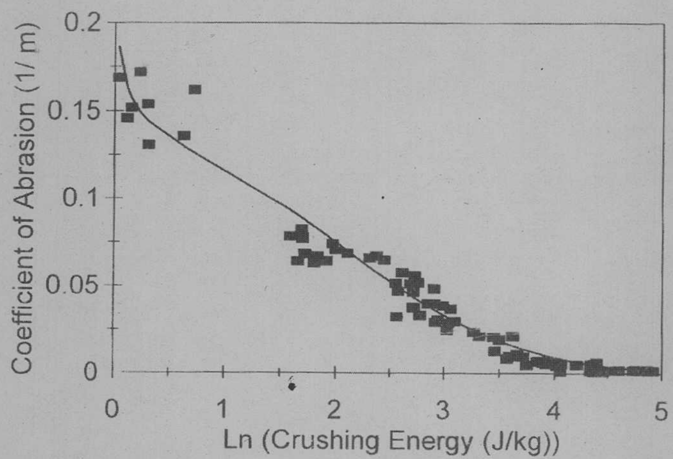

Fig. 5. Coefficient abrasion of dry, immobile clods and crust as a function of natural logarithm of crushing energy (Hagen et al., 1992).

from abrasion, F_{ani} is mass fraction saltation impacting clods and crust, and C_{ani} is coefficient of abrasion (m^{-1}).

An index of two was used in Eq. 11 because, in general, only two targets, exposed clods and crust, must be considered. Other targets, such as residue and rocks, have a C_{ani} near zero. The first term, (1 - $Sfss_{an}$), is the fraction of abraded mass that is of saltation/creep-size. Values of $Sfss_{an}$ for some Kansas soils have been measured and ranged from 0.14 to 0.27, depending on soil texture (Mirzamostafa, 1996). The middle, bracketed term on the right-hand-side of Eq. 11 represents the total soil abraded from clods and crust, as confirmed by wind tunnel experiments (Hagen, 1991). Values for C_{ani} also have been measured for a range of soils and related to clod crushing energy (Fig. 5, Hagen *et al.*, 1992). The final term in Eq. 11 is the mass fraction entrained in the air stream. The entrainment rate of this newly-created saltation/creep is assumed to be similar to that of loose, saltation/creep-size aggregates already present on the surface, and that the entrainment approaches zero at transport capacity.

A sink for the saltation/creep discharge occurs when these aggregates are broken into suspension-size and carried away by convection and diffusion (Mirzamostafa *et al.*, 1998). This effect is simulated as

$$Gss_{bk} = C_{bk}\,(q - q_s) \qquad ...12$$

where,
C_{bk} is coefficient of breakage (m^{-1}), and
q_s is discharge of primary (non-breakable) sand particles (kg m^{-1} s^{-1}).

The saltation/creep aggregates are more stable than the surface clods and crust, so measured abrasion coefficients average about nine times more than the breakage coefficients on the same soils (Mirzamostafa, 1996). The wind tunnel experiments also demonstrated that the breakage coefficient remained constant during breakdown of the aggregates to primary particles. The means and variances of these coefficients are related to soil texture. Given q, values for q_s can be estimated directly from soil sand content.

Another sink term is the removal of saltation/creep from the air stream by trapping mechanisms (Hagen and Armbrust, 1992). Surface trapping and plant interception can be simulated as

$$G_{tp} = C_t \left(1 - \frac{q_{cp}}{q_{en}}\right) q + C_i q \qquad ..13$$

where,
C_t is coefficient of surface trapping (m^{-1}),
C_i is coefficient of plant interception (m^{-1}),
and q_{cp} is transport capacity of the surface, when 40% or more is armored (kg m^{-1} s^{-1}).

When erosive winds cross rough surfaces, such as tillage ridges, that are highly erodible, large amounts of soil are entrained, but a portion of the entrained saltation/creep is often trapped in succeeding downwind furrows. This phenomenon results in a local rearrangement of the surface and reduces net removal of the entrained soil. Our conventionally defined transport capacity, q_{en}, is based on the threshold velocity where erosion begins. But, when trapping of saltation/creep occurs on rough surfaces, one may hypothesize that q_{en} has been exceeded, and that the true transport capacity of the surface is some value, q_{cp}, that is less than q_{en}. However, q_{en} still appears to be the appropriate limiting value to drive the emission process, because more soil is emitted than can be transported from the local area.

Thus, the first term on the right-hand-side of Eq. 13 simulates trapping of saltation/creep by surface roughness. The true transport capacity of the surface, q_{cp}, is based on the threshold friction velocity needed to remove saltation/creep from the furrows. It is calculated using threshold friction velocity for a given roughness at the level of clod and crust cover of the surface but with a minimum set at 40% of the surface armored. Under this condition, wind tunnel observations show that loose material is removed, but minimal local trapping of saltation/creep occurs.

The second term of Eq. 13 represents interception of saltation/creep by standing plant stalks or other near-surface plant parts. This term arises because for a given soil surface friction velocity, more transport occurs without than with stalks. This term also is used to assign a higher transport capacity for wind direction parallel to crop rows than for wind direction perpendicular to rows. For saltation normal to the row direction, interception can reduce transport capacity 5 to 10% or more. Comparisons to measured data have been reported previously (Hagen and Armbrust, 1994).

Suspension Discharge

Based on conservation of mass in a control volume that extends to the top of the dust cloud, a one-dimensional, quasi-steady state equation for the physical processes generating the suspension component is

$$\frac{dqss}{dx} = Gss_{en} + Gss_{an} + Gss_{bk} - Gss_{tp},\ u{*}>u{*}_t \qquad ...14$$

or

$$\frac{dqss}{dx} = GSS_{dp},\quad u{*} < u{*}_t \qquad ...15$$

where,
qss is horizontal suspension component discharge (kg m^{-1} s^{-1}). The terms on the right hand side of Eqs. 14 and 15 are all vertical fluxes (kg m^{-2} s^{-1}). Gss_{en} is emission flux of loose, suspension-size aggregates, Gss_{an} is flux of suspension-size aggregates created by abrasion of clods and crust, Gss_{bk} is flux of suspension-size

aggregates created by breakage of saltation/creep-size aggregates, Gss_{tp} is flux from trapping suspension-size aggregates, and Gss_{dp} is flux (deposition) of suspension-size aggregates above a non-eroding surface.

The source and sink terms for the suspension component can be simulated by the equations that follow. For direct emission of loose, suspension-size material by 'splash' impacts and aerodynamic forces

$$Gss_{en} = SFss_{en}\, C_{en}\, (q_{en} - q) + C_m\, q \qquad ...16$$

where,
C_m is a coefficient of mixing, value about $(0.0001\ SFss_{en})\ (m^{-1})$.

Below transport capacity, the driving force causing the emission flux of suspension-size soil is assumed to be similar to that in Eq. 10 causing the saltation/creep emission flux. This assumption is supported by wind tunnel measurements that show a mixture of suspension-size aggregates and a mixture of saltation-size have about the same threshold velocities (Chepil, 1951).

However, two additional assumptions are inherent in Eq. 16. The first is that the loose components of saltation/creep and suspension-size aggregates occur as a uniform mixture in the field. As a consequence, during simple net emission, the suspension fraction emitted with the saltation/creep remains the same as it was in the soil. Hence, the suspension fraction can be estimated as

$$SFss_{en} = \frac{SFss}{SFer} \qquad ...17$$

where,
SFss is soil mass fraction of loose, suspension-size less than about 0.1 mm, and SFer is soil mass fraction of loose, erodible-size, less than about 2.0 mm.

The second assumption in Eq. 16 is that an additional small amount of suspension-size aggregates that are disturbed by the saltation impacts also are entrained, because transport capacity for the suspension component generally is not limiting. The result of this process is gradual depletion of the loose, suspension-size aggregates at the surface. However, when net emission of suspension-size exceeds net emission of saltation/creep-size aggregates, the latter soon dominate the surface area and absorb the impacts, so the process tends to be self-limiting. For suspension flux created by abrasion of clods and crust,

$$Gss_{an} = SFss_{an} \sum_{1}^{2} (F_{ani}\ C_{ani})\ q \qquad ...18$$

Additional discussion and measurements of this source term were reported by Mirzamostafa *et al.* (1998).

For the source of suspension flux created by breakage of saltation/creep aggregates, the term is the same as the sink term in the saltation/creep equation and simulated as

$$Gss_{bk} = C_{bk}\ (q - q_s) \qquad ...19$$

Breakage from impact on immovable targets is assumed to come only from the impacting saltation/creep alone. Breakage coefficients for saltation-size aggregates have been measured in the wind tunnel (Mirzamostafa *et al.*,1998). But the breakage component from impacts on other saltation/creep is assumed to come from both the impacting and target aggregates. Breakage from impact on a mobile target is less likely than breakage from impact on immobile targets. However, these assumptions need further experimental verification.

When exiting the biomass canopy, a small portion of the suspension component also may be trapped or intercepted by plants similar to interception of saltation/creep. This effect likely is relatively small in the sparse biomass populations that permit erosion. Nevertheless, additional experimental data are needed to quantify this process.

Another, sink term for trapping of suspension flux occurs when the suspension discharge passes over areas without active saltation to maintain the suspension flux from the surface. Typically, this implies the presence of a vegetated, water, or rough armored surface. The largest suspension particles, 0.05 to 0.10 mm, comprize roughly half the mass of the suspension discharge (Chepil, 1957; Zobeck and Fryrear, 1986). Through diffusion and settling, they move rapidly toward non-eroding surfaces in the simulation region, which serve as sinks. The process is simulated as

$$Gss_{d\,p} = C_{d\,p}\ (qss - qss_o),\ \ qss > 0.5 qss_o \quad ...20$$

where,

qss_o is maximum value of qss entering deposition region (kg m^{-1} s^{-1}), and C_{dp} is coefficient of deposition of suspension-size (m^{-1}). The maximum value of C_{dp} is about 0.02, but less for smooth surfaces or large upwind areas that produce high dust clouds, thus moving a large portion of the soil beyond the local deposition area. Others have shown the deposition flux to be a function of surface roughness, surface retention characteristics, and particle size (Schack *et al.*, 1985; Reynolds, 2000). Thus, the preceding equation is only a rough approximation of near-field deposition. Additional research is needed to provide predicted concentration profiles and size distributions of suspension-size soil that occur over the range of wind-erodible soils.

As illustrated by the preceding equations, generation of the suspension component is intimately associated with the saltation/creep component. Analytic solutions for these linked saltation/creep and suspension discharge differential equations have been developed (Hagen *et al.*, 1999) and validated using measured data from small fields (Hagen, 2001a). The suspension component has a large transport capacity, and the suspension generation processes occur over the entire eroding area. Thus, on uniform, eroding areas suspension discharge should continually increase in the downwind direction. Data collected at Owens Lake in California illustrate nicely the differing response of saltation/creep and suspension discharge on a large area (Fig. 6). In these data, the saltation/creep transport capacity occurs at about 660 m downwind, while there is a continual increase in the suspension discharge in the downwind direction. Although only a portion of the suspension component was collected in the samplers, it still greatly exceeded the saltation/creep transport capacity at 1600 m downwind.

PM_{10} and $PM_{2.5}$ Discharge

The smallest particles in the suspension discharge, particulate matter with aerodynamic diameters less than 10 µm (PM_{10}) and less than 2.5 µm ($PM_{2.5}$), are considered health hazards in the United States (Ostro and Chestnut, 1998). Substantial amounts of these fine particles are generated during wind erosion, and high PM_{10} concentrations cause some locations to be in non-compliance with clean air act standards

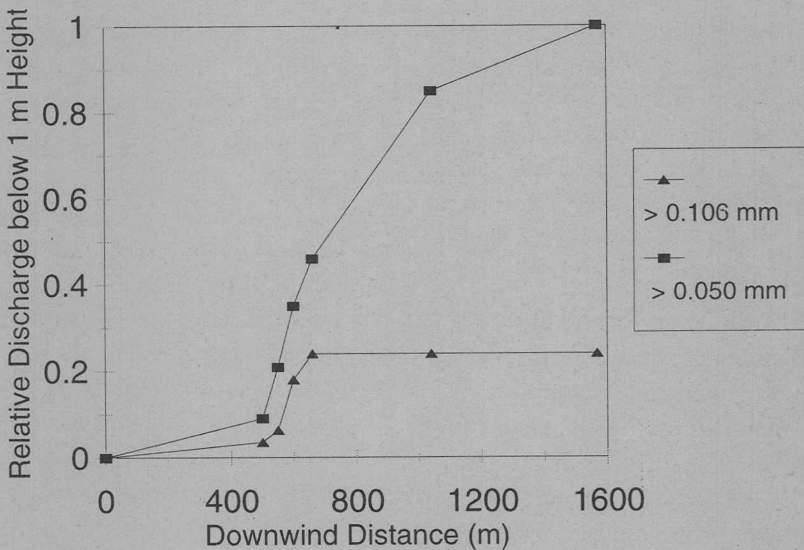

Fig. 6. Relative discharge below 1 m as a function of downwind distance for saltatin/creep aggregate <0.106 mm and total aggregates <0.050 mm in diameter at Owens Lake, CA. The difference between the lines represents part of the suspension discharge (Gillette et al., 1997).

(Claiborn *et al.*, 2000). PM_{10} and $PM_{2.5}$ are generated by the same processes as the other suspension-size particles, so the process equations discussed in the prior section also can be applied to generation of fine PM particles, but with different parameters. Parameters for their simulation have been measured for some soils (Hagen *et al.*, 1996; Hagen and James, 1998; Hagen, 2001b).

Proposed regulations would require $PM_{2.5}$ concentrations to be about one-third that of PM_{10} concentrations (U.S. EPA, 1996). During wind erosion, the highest ratio of $PM_{2.5}/PM_{10}$ is produced by the breakage process (Hagen and James, 1998). For a range of soils subjected to breakage, the ratio averaged 0.154, but increased with saltation-size sand/clay ratio of the parent soils (Fig. 7). The $PM_{2.5}/PM_{10}$ ratio also was inversely related to the annual precipitation (100 to 800 mm range) at sampling sites in the western U.S. Using both sand/clay ratio and annual precipitation in a regression equation gave a coefficient of determination, R^2, of 0.53. These data suggest that the proposed $PM_{2.5}$ standard should not be more difficult to attain than the PM_{10} standard when local wind erosion is the only $PM_{2.5}$ source affecting the target population.

Conclusions

In prior decades, wind erosion prediction and the design of control measures on agricultural lands often depended on using a series of lumped factors. The lumped factors usually embodied several individual erosion processes. Hence, wind tunnel measurements of factor values that were directly applicable to the field were often problematic. However,

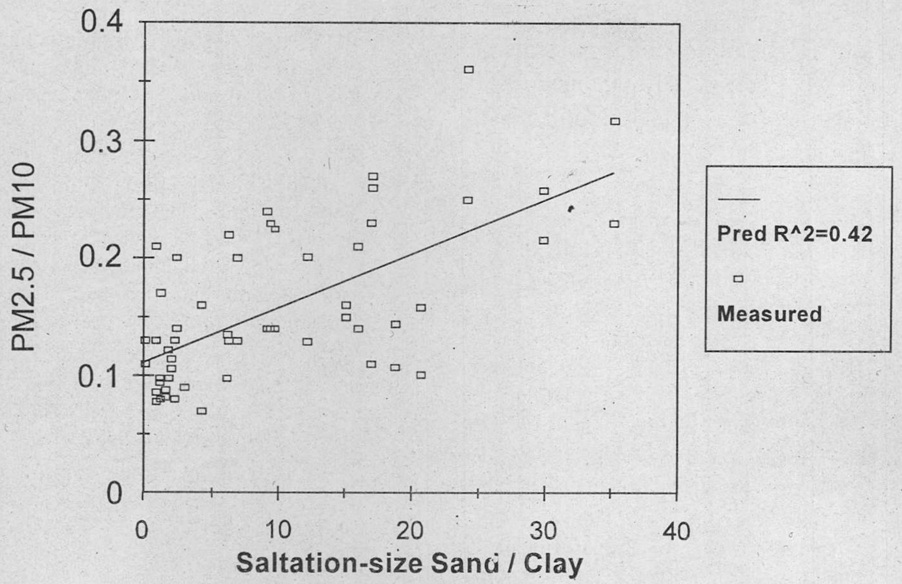

Fig. 7. Ratio of $PM_{2.5}/PM_{10}$ created by brakage of saltation-size aggregates as a function of the sand/clay ratio of the present soil for sand >0.1 mm diameter (Hagen, 2001b).

during the last decade considerable progress has been made in formulating equations to represent individual erosion processes that constitute the sources and sinks for eroding soil. The soil state and the individual erosion processes can be used to delineate measurable soil temporal properties that control wind erosion.

The equations describing both the wind erosion processes and their boundary conditions are physically-based, and most of the associated coefficients can be measured individually in wind tunnels. Boundary conditions for the processes include threshold friction velocities and transport capacity of saltation/creep. Sources of saltation/creep discharge include entrainment of loose aggregates and abrasion of immobile clods and crust. Sinks for saltation/creep discharge include trapping by surface roughness, interception by standing biomass and breakage to suspension-size. Similarly, sources for suspension discharge include entrainment of loose aggregates, abrasion of clods and crust, and breakage of saltation/creep aggregates. Sinks for suspension include interception by standing biomass and deposition on downwind immobile surfaces.

Recently, the individual processes have been described by linked differential equations that can estimate erosion for a wide range of surface conditions. This linking allows one to explore the interactions among the various erosion processes. The erosion generated by the individual processes has also been partitioned to the separate transport modes of saltation/creep and suspension. Current research has begun to delineate the PM_{10} and $PM_{2.5}$ generation potential of various soils. Separating the soil discharge leaving a field by direction and into components of saltation/creep, suspension, PM_{10} and $PM_{2.5}$ can greatly enhance utility of model predictions for estimating off-site erosion impacts.

References

Anderson, R.S., Sorenson, M. and Willets, B.B. 1991. A review of recent progress in our understanding of aeolian sediment transport. *Acta Mechanica (Supplement)* 1: 1-19.

Armbrust, D.V. and Bilbro, J.D. 1997. Relating plant canopy characteristics to soil transport capacity by wind. *Agronomy Journal* 89(2): 157-162.

Bagnold, R.A. 1941. T*he Physics of Blown Sand and Desert Dunes*. Methuen, New York, USA.

Boyd, D.W., Skidmore, E.L. and Thompson, J.G. 1983. A soil-aggregate crushing-energy meter. *Soil Science Society of America Journal* 47(2): 313-316.

Chepil, W.S. 1951. Properties of soil which influence wind erosion. IV. State of dry aggregate structure. *Soil Science* 75(2): 387-401.

Chepil, W.S. 1957. Sedimentary characteristics of duststorms: III. Composition of the suspended dust. *American Journal of Science* 255: 206-213.

Chepil, W.S. 1958. *Soil Conditions that Influence Wind Erosion*. Technical Bul. No. 1185, 40 pp., USDA, Washington, DC.

Chepil, W.S. and Woodruff, N.P. 1957. Sedimentary characteristics of dust storms: II. Visibility and dust concentration. *American Journal of Science* 255: 104-114.

Chepil, W.S. and Woodruff, N.P. 1963. The physics of wind erosion and its control. *Advances in Agronomy* 15: 211-302.

Claiborn, C.S., Finn, D., Larson, T.V. and Koening, J.Q. 2000. Windblown dust contributes to high PM2.5 concentrations. *Journal of Air & Waste Management Association* 50: 1440-1445.

Draxler, R.R., Gillette, D.A., Kirkpatrick, J.S. and Heller, J. 2001. Estimating PM10 concentrations from dust storms in Iraq, Kuwait, and Saudi Arabia. *Atmospheric Environment* 35: 4315-4330.

Fryrear, D.W., Saleh, A. and Bilbro, J.D. 1998. A single event erosion model. *Transactions of the American Society of Agricultural Engineers* 34(1): 155-160.

Gares, P.A. 1988. Factors affecting eolian sediment transport in beach and dune environments. *Journal of Coastal Research*, Special Issue 3: 121-126.

Gillette, D.A., Fryrear, D.W., Xiao, J.B., Stockton, P., Ono, D., Helm, P.J., Gill, T.E. and Ley, T. 1997. Large-scale variability of wind erosion mass flux rates at Owens Lake. 1. Vertical profiles of horizontal mass fluxes of wind-eroded particles with diameter greater than 50 μm. *Journal of Geophysical Research* 102(D22): 25,977-25,987.

Greeley, R. and Iversen, J.D. 1985. *Wind as a Geological Process on Earth, Mars, Venus, and Titan*. Cambridge University Press, New York.

Hagen, L.J. 1991. Wind erosion mechanics: Abrasion of aggregated soil. *Transactions of the American Society of Agricultural Engineers* 34(4): 831-837.

Hagen, L.J. 1995. Erosion submodel. In *Wind Erosion Prediction System Technical Description*. Proceedings of WEPP/WEPS Symposium, pp. E1-E47, August 9-11, Des Moines, IA. Soil and Water Conservation Society, Ankeny, IA.

Hagen, L.J. 1996. Crop residue effects on aerodynamic processes and wind erosion. *Theoretical and Applied Climatology* 54: 39-46.

Hagen, L.J. 1999. Wind erosion prediction system: Erosion submodel. In *Wind Erosion - An International Symposium/Workshop* (Eds. E.L. Skidmore and J. Tatarko), June 3-5, 1997, USDA, ARS, Wind Erosion Research Unit, Kansas State University, Manhattan, KS.

Hagen, L.J. 2001a. Validation of the wind erosion prediction system (WEPS) erosion submodel on small cropland fields. In *Soil Erosion Research for the 21st Century* (Eds. J.C.I. Ascough and D.C. Flanagan), pp. 479-482. Proceedings of the International Symposium. ASAE, St Joseph, MI, USA., Honolulu, Hawaii, USA.

Hagen, L.J. 2001b. Fine particulates (PM10 and PM2.5) generated by breakage of mobile aggregates during simulated wind erosion. *American Society of Agricultural Engineers Meeting Paper No. 01-2072*, St. Joseph, MI.

Hagen, L.J. 2001c. Assessment of wind erosion parameters using wind tunnels. In *Proceedings of 10th International Soil Conservation*

Organization Conference, May 23-28, 1999, Purdue Univ.,West Lafayette, IN (in press).

Hagen, L.J. and Armbrust, D.V. 1992. Aerodynamic roughness and saltation trapping efficiency of tillage ridges. *Transactions of the American Society of Agricultural Engineers* 35(5): 1179-1184.

Hagen, L.J. and Armbrust, D.V. 1994. Plant canopy effects on wind erosion saltation. *Transactions of the American Society of Agricultural Engineers* 37(2): 461-465.

Hagen, L.J. and James, D.E. 1998. The PM-10 production potential of soils in the Las Vegas Valley of Nevada. In *Dust, Aerosols, Loess Soils and Global Change* (Ed. A.J.Busaca), Washington State Univ. College of Agriculture and Home Economics, pp. 45-48. Miscellaneous Pub. No. MISC0190, Pullman, WA.

Hagen, L.J., Mirzamostafa, N. and Hawkins, A. 1996. PM-10 generation by wind erosion. In *International Conference on Air Pollution from Agricultural Operations*, pp.79-86. Feb. 7-9, Kansas City, MO.

Hagen, L.J., Schroeder, B. and Skidmore, E.L. 1995. A vertical soil crushing-energy meter. *Transactions of the American Society of Agricultural Engineers* 38(3): 711-715.

Hagen, L.J., Skidmore, E.L. and Saleh, A. 1992. Wind erosion: prediction of aggregate abrasion coefficients. *Transactions of the American Society of Agricultural Engineers* 35(6): 1847-1850.

Hagen, L.J., Wagner, L.E. and Skidmore, E.L. 1999. Analytical solutions and sensitivity analyses for sediment transport in WEPS. *Transactions of the American Society of Agricultural Engineers* 42(6): 1715-1721.

Iversen, J.D. and White, B.R. 1982. Saltation threshold on Earth, Mars, and Venus. *Sedimentology* 29: 111-119.

Lettau, K. and Lettau, H.H. 1978. Experimental and micro-meteorological field studies of dune migration. In *Exploring the World's Driest Climate* (Eds. H.H. Lettau and K. Lettau), pp. 110-147. Institute for Environmental Studies, IES Report 101, University of Wisconsin-Madison, WI.

Leys, J. 1999. Wind erosion on agricultural land. In *Aeolian Environments, Sediments, and Landforms* (Eds. A.S. Goudie, I. Livingstone, and S. Stokes), pp. 143-166. John Wiley & Sons, New York.

Lyles, L., Schrandt, R.L. and Schmeidler, N.F. 1974. How aerodynamic roughness elements control sand movement. *Transactions of the American Society of Agricultural Engineers* 17(1): 134-139.

Marshall, J.K. 1971. Drag measurements on roughness arrays of varying density and distribution. *Agricultural Meteorology* 8: 269-292.

Marticorena, B. and Bergametti, G. 1995. Modeling the atmospheric dust cycle: 1. Design of a soil-derived dust emission scheme. *Journal of Geophysical Research* 100(D8):16,415-16,430.

Marticorena, B., Bergametti, G., Gillette, D.A. and Belnap, J. 1997. Factors controlling threshold friction velocity in semiarid and arid areas of the United States. *Journal of Geophysical Research* 1 102 (D19): 23,277-23,287.

McKenna-Neuman, C. and Nickling, W.G. 1989. A theoretical and wind tunnel investigation of the effect of capillary water on the entrainement of sediment by wind. *Canadian Journal of Soil Science* 69: 79-96.

Mirzamostafa, N. 1996. Suspension component of wind erosion. *Ph.D. Dissertation*, Kansas State University, Manhattan, KS, 126 p.

Mirzamostafa, N., Hagen, L.J., Stone, L.R. and Skidmore, E.L. 1998. Soil and aggregate texture effects on suspension components from wind erosion. *Soil Science Society of America Journal* 62: 1351-1361.

Ostro, B. and Chestnut, L. 1998. Assessing the health benefits of reducing particulate matter air pollution in the United States. *Environmental Research* 76: 94-106.

Potter, K.N. 1990. Estimating wind-erodible materials on newly crusted soils. *Soil Science* 150(5): 771-776.

Raupach, M.R. 1992. Drag and drag partition on rough surfaces. *Boundary Layer Meteorology* 60: 375-395.

Retta, A., Armbrust, D.V. and Hagen, L.J. 1996. Partitioning biomass in the crop submodel of WEPS (Wind Erosion Prediction System). *Transactions of the American Society of Agricultural Engineers* 39(1): 145-151.

Reynolds, A.M. 2000. Prediction of particle deposition onto rough surfaces. *Agricultural and Forest Meteorology* 104: 107-118.

Saleh, A. and Fryrear, D.W. 1995. Threshold wind velocities of wet soils as affected by wind blown sand. *Soil Science* 160(4): 304-309.

Saxton, K.E., Chandler, D., Stetler, L., Lamb, B., Claiborn, C. and Lee, B.H. 2000. Wind erosion and fugitive dust fluxes on agricultural lands in the Pacific Northwest. *Transactions of the American Society of Agricultural Engineers* 43(3): 623-630.

Schack, C.J., Pratsinis, S.E. and Friedlander, S.K. 1985. A general correlation for deposition on suspended particles from turbulent gases to completely rough surfaces. *Atmospheric Environment* 19(6): 953-960.

Shao, Y., Raupach, M. and Leys, J.F. 1996. A model for predicting aeolian sand drift and dust entrainment on scales from paddock to region. *Australian Journal of Soil Research* 34: 309-342.

Skidmore, E.L. and Layton, J.B. 1992. Dry-soil aggregate stability as influenced by selected soil properties. *Soil Science Society of America Journal* 56(1): 557-561.

U.S. EPA. 1996. National ambient air quality standards for particulate matter: Proposed decision. 40 CFR 50 61(241), Federal Register 61(241).

Van Dijk, P.M., Arens, S.M. and Van Boxel, J.H. 1999. Aeolian processes across transverse dunes. II. Modeling the sediment transport and profile development. *Earth Surface Processes and Landforms* 24: 319-333.

Wagner, L.E. and Hagen, L.J. 1992. Relationship between shelter angle and surface roughness and cumulative sheltered storage depth. In *Proceedings of the International Wind Erosion Workshop of CIGR* (Eds. J. Karacsony and G. Szalai), Section I, 10 pp. September 10-12. 1991, Budapest, Hungary. V.

White, B.R. and Tsoar, H. 1998. Slope effect on saltation over a climbing sand dune. *Geomorphology* 22: 159-180.

Woodruff, N.P. and Siddoway, F.H. 1965. A wind erosion equation. *Soil Science Society of America Proceedings* 29(5): 602-608.

Zobeck, T.M. 1989. Fast-Vac a vacuum system to rapidly sample loose granular material. *Transactions of the American Society of Agricultural Engineers* 32(4): 1316-1318.

Zobeck, T.M. and Fryrear, D.W. 1986. Chemical and physical characteristics of windblown sediment I. Quantities and physical characteristics. *Transactions of the American Society of Agricultural Engineers* 29(4): 1032-1036.

Zobeck, T.M. and Onstad, C.A. 1987. Tillage and rainfall effects on random roughness: A review. *Soil & Tillage Research* 9: 1-20.

Zobeck, T.M. and Popham, T.W. 1992. Influence of microrelief, aggregate size, and precipitation on soil crust properties. *Transactions of the American Society of Agricultural Engineers* 35(2): 487-492.